Science Bulletin 68 (2023) 1306–1316

Contents lists available at ScienceDirect

Science Bulletin

journal homepage: www.elsevier.com/locate/scib

Article

Mapping global distribution of mangrove forests at 10-m resolution

Mingming Jia [a,b], Zongming Wang [b,*], Dehua Mao [b], Chunying Ren [b], Kaishan Song [b], Chuanpeng Zhao [b], Chao Wang [d], Xiangming Xiao [e], Yeqiao Wang [c,*]

[a] International Research Center of Big Data for Sustainable Development Goals, Beijing 100094, China
[b] Key Laboratory of Wetland Ecology and Environment, Northeast Institute of Geography and Agroecology, Chinese Academy of Sciences, Changchun 130102, China
[c] Department of Natural Resources Science, University of Rhode Island, Kingston RI 02881, USA
[d] State Key Laboratory of Information Engineering in Surveying, Mapping and Remote Sensing, Wuhan University, Wuhan 430079, China
[e] Department of Microbiology and Plant Biology, Center for Earth Observation and Modeling, University of Oklahoma, Norman OK 02881, USA

ARTICLE INFO

Article history:
Received 21 November 2022
Received in revised form 1 April 2023
Accepted 6 April 2023
Available online 10 May 2023

Keywords:
Remote sensing
Sentinel-2
Object-based image analysis
World heritage sites
Ramsar convention sites

ABSTRACT

Mangrove forests deliver incredible ecosystem goods and services and are enormously relevant to sustainable living. An accurate assessment of the global status of mangrove forests warrants the necessity of datasets with sufficient information on spatial distributions and patch patterns. However, existing datasets were mostly derived from ~30 m resolution satellite imagery and used pixel-based image classification methods, which lacked spatial details and reasonable geo-information. Here, based on Sentinel-2 imagery, we created a global mangrove forest dataset at 10-m resolution, namely, High-resolution Global Mangrove Forests (HGMF_2020), using object-based image analysis and random forest classification. We then analyzed the status of global mangrove forests from the perspectives of conservation, threats, and resistance to ocean disasters. We concluded the following: (1) globally, there were 145,068 km^2 mangrove forests in 2020, among which Asia contained the largest coverage (39.2%); at the country level, Indonesia had the largest amount of mangrove forests, followed by Brazil and Australia. (2) Mangrove forests in South Asia were estimated to be in the better status due to the higher proportion of conservation and larger individual patch size; in contrast, mangrove forests in East and Southeast Asia were facing intensive threats. (3) Nearly, 99% of mangrove forest areas had a patch width greater than 100 m, suggesting that nearly all mangrove forests were efficient in reducing coastal wave energy and impacts. This study reports an innovative and up-to-date dataset and comprehensive information on mangrove forests status to contribute to related research and policy implementation, especially for supporting sustainable development.

1. Introduction

Mangrove forests are one of the most biologically diverse and productive ecosystems on Earth [1,2]. Globally, approximately 75% of low-lying tropical coastlines receiving freshwater drainage support mangrove systems [3]. They provide coastal area protection by attenuating wave energy and storm surges and stabilizing shorelines from flooding and erosion [4–6]. Mangrove forests are also important for climate mitigation due to their capacity for efficient carbon sequestration and storage [7–9]. Globally, hundreds of millions of people directly rely on mangrove forests to provide a variety of resources to local communities [10–12]. Therefore, mangrove forests play an essential role in a sustainable future for human beings [13]. The unique and important ecosystem functions warrant the necessity of detailed spatial information on global mangrove forests to provide essential information for related scientific research and coastal management, as well as to facilitate the implementation of sustainable development [14,15].

Mangrove forests growing along coastlines always appear in narrow strips and small patches [16]. Thus, current existing global mangrove forest datasets may be insufficient to support the increasing requirements of in-depth scientific research and precision management. Existing datasets can be generally divided into two categories, i.e., statistical reports from various sources and maps derived from satellite images. The statistical reports were collective efforts by various management and research institutions and international organizations published from 1981 to 2020 [14,17–21]. These reports offered a glance at areas of mangrove forests in various administrative units but lacked spatial distribution details.

* Corresponding authors.
E-mail addresses: zongmingwang@iga.ac.cn (Z. Wang), yqwang@uri.edu (Y. Wang).

https://doi.org/10.1016/j.scib.2023.05.004
2095-9273/

Satellite remote sensing, which is considered accurate, rapid, and cost effective, provides a solution to produce globally consistent mangrove forests maps [15,22,23]. One of the earliest global mangrove forests mapping datasets was the World Mangrove Atlas, which was published in 1997 [24,25]. The atlas was surveyed and mapped from a range of different data sources, such as thematic maps, literature, and remote sensing images. The first global consistent mangrove forest dataset with more spatial and thematic details was published in 2011 [26]. Then, Hamilton and Casey [27] interpreted the extents of world's mangrove forests during 2000–2012. Furthermore, Thomas et al. [28] and Bunting et al. [29] mapped mangrove deforestation and conversions during 1996–2016 using L-band SAR and Landsat imagery, respectively. These datasets were named Global Mangrove Watch (GMW). The above maps and datasets were all derived from ~30 m resolution remote sensing images in which small mangrove patches could be omitted [30]. Recently, Bunting et al. updated the GMW dataset to GMW v2.5 by revising 204 regions using Sentinel-2 imagery [30] and then solely used L-band SAR to detect changes from v2.5 and built GMW v3.0 [31]. However, due to the limitations of data sources and classification methods, these datasets still contained regions with considerable errors. The errors can largely affect the evaluations of global mangrove forests status. Inconsistencies in data quality, cartographic standards, modeling methods, and spatiotemporal coverage of data sources often produce different results, resulting in difficulties in conducting accurate, reliable, and comprehensive socioeconomic assessments [32].

In addition to spatial distributions, previous global-scale mangrove studies have focused on rates and drivers of deforestation [28,33], biomass and carbon estimation [27,34,35], fragmentation [36], and climate change [37–40]. Most recently, the Global Mangrove Alliance (GMA) published a report of the State of the World's Mangroves (https://www.mangrovealliance.org/mangrove-forests/), which mentioned little about mangrove conservation and threats. However, spatial details were not presented. Furthermore, models indicated that abelt of mangrove forests with a 100 m width could significantly reduce wave energy [41,42]. Previous studies also indicated that mangrove patches with a width greater than 1500 m would reduce 1-m high waves to 0.05 m [43,44]. Thus, the patch widths are strongly related to the capacity of mangrove forests in ocean disaster resilience and coastal property protection. However, a specific analysis of global mangrove forests as coastal protectors does not exist. The essential barrier is the lack of finer resolution global mangrove forests datasets with patches of reasonable geo-information.

To solve the abovementioned issues, in this study, we first produced an up-to-date high spatial resolution (10 m) global mangrove forest dataset, namely, High-resolution Global Mangrove Forests (HGMF_2020), based on object-based image analysis (OBIA) and a massive collection of Sentinel-2 images acquired during 2020. Second, we analyzed the geographical characteristics and patch patterns of global mangrove forests. Finally, we discussed the status of global mangrove forests conservation and threats. The HGMF_2020 dataset and our state-of-the-art global mangrove forests analyses provide baseline data for scientific research to provide decision-makers with an accessible reference for designing sustainable mangrove management policies.

2. Materials and methods

2.1. Sentinel-2 satellite imagery and auxiliary data

The Sentinel-2 MultiSpectral Instrument (MSI) sensor contains 13 spectral bands. In this study, four spectral bands (Bands 2, 3, 4, and 8) at 10 m and six bands (Bands 5, 6, 7, 8A, 11, and 12) at 20 m spatial resolutions were chosen to identify mangrove forests and other land covers. This study used 124,000 scenes of Sentinel-2 Level-2A products, which covered the entire study area within 2020.

For other auxiliary data, global protected areas of mangrove forests were downloaded from the official websites of the Ramsar Convention on Wetlands (https://www.ramsar.org/), World Heritage Convention (https://whc.unesco.org/), and Protected Planet (https://www.protectedplanet.net/en), which contain the World Database on Protected Areas, Global Database on Protected Area Management Effectiveness, World Database on other effective area-based conservation measures, and a wealth of national and local reserves.

To obtain globally evenly distributed validation samples, three steps were conducted by an independent team. First, samples were downloaded from two global crowdsourced datasets, i.e., Collect Earth (https://openforis.org/tools/collect-earth) and Global Biodiversity Information Facility (https://www.gbif.org/). Then, to ensure the credibility of crowdsourced samples, we visually examined all these samples in Google Earth. Finally, for regions with sparse ground samples, we visually interpreted ground samples from submeter resolution imagery in Google Earth. We generated the number of ground samples for mangroves and non-mangroves in a 1:3 ratio. In total, 21,704 and 60,243 points were collected as ground truth samples for the categories of mangrove forest and others, respectively. The distributions of these samples are illustrated in Fig. S1 (online).

2.2. Methodology of mangrove forest classification

To obtain robust spatial information on mangrove forests, we developed a classification methodology that contained three steps: (1) identifying specific study areas based on four available global-scale mangrove datasets; (2) building global Sentinel-2 composite images in the Google Earth Engine (GEE) platform; and (3) applying OBIA and random forest (RF) classification to map mangrove forests. To undertake the processing, study areas were divided into 144 project tasks that were grouped into $1^\circ \times 1^\circ$ tiles, GEE was used to composite and download images for each task, and eCognition software was used to segment images, run RF classification, and conduct postprocessing. Finally, ArcGIS was used to merge all the classification results. Fig. 1a shows the workflow for mapping mangrove forests. We also provided a typical application in Dongzhaigang, China (Fig. 1b–d).

(i) Identifying specific study areas. First, we merged four large-scale mangrove datasets to generate a baseline map as the reference. We then created 1-km buffers for all patches of the baseline map. Finally, we generated the study areas by combining the patches in the baseline map and their buffers. The areal extent of the study area was 637,844 km^2. Mangrove datasets used as references in this step included Global Mangrove Forests Distribution (GMFD) [26], Global Mangrove Watch (v2.0, v2.5 and v3.0) [29–31], Continuous Global Mangrove Forest Cover for the 21st Century (2000–2012) (CGMFC-21) [27], and CAS_Mangroves [45,46].

(ii) Building Sentinel-2 composite images. To rapidly and robustly acquire images suitable for mangrove forest mapping, we conducted a maximum spectral index composite (MSIC) process to produce working images. For each location of an individual pixel, the MSIC selected a pixel with the maximum spectral index in a time-series image collection and then composited a new image. In this study, the normalized difference vegetation index (NDVI) [47] was selected to conduct the MSIC, which ensured that pixels in a composite image represented the highest NDVI values. We named the

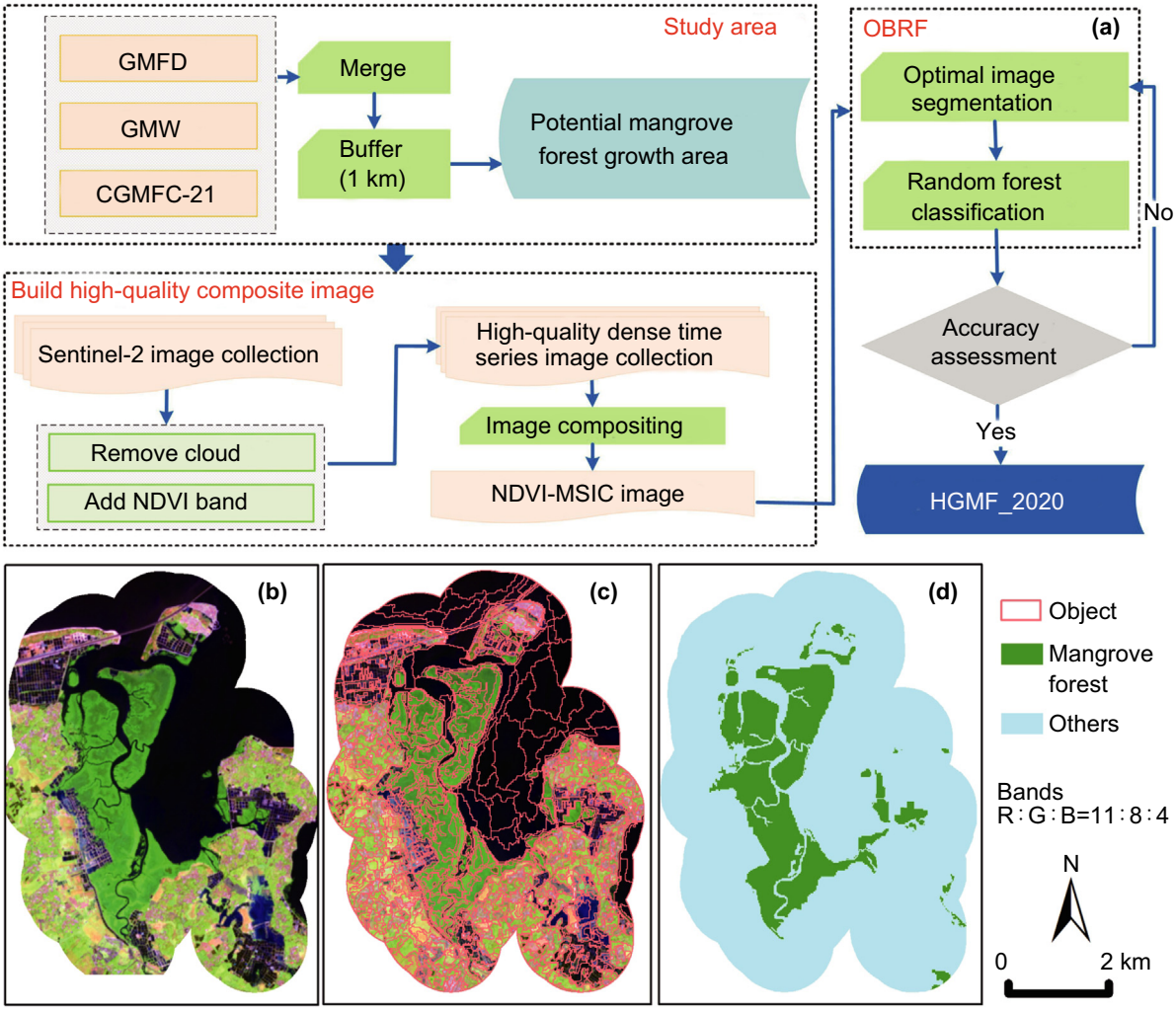

Fig. 1. Workflow of mapping mangrove forests and a typical application in Dongzhaigang, China. (a) Workflow of the mapping approach; (b) NDVI-MSIC image of Dongzhaigang; (c) object segmentation result; (d) object-based image analysis and random forest (OBRF) classification result. R: the red channel, G: the green channel, B: the blue channel.

composite images NDVI-MSIC images (Fig. 1b). All bands in the NDVI-MSIC images were then resampled to a 10-m resolution. The procedure was performed in the GEE platform, and the code can be found in the Resource Availability section.

(iii) Classification of mangrove forest and other land covers. The OBIA was successfully applied to map mangrove forests and other wetlands [48]. Image segmentation is the first and most important step of OBIA, and it can reduce "within-class" variation by segmenting images into objects. The RF classifier is an ensemble machine learning method that constructs a number of decision trees to conduct classification. The RF classifier has been proven efficient in mapping mangrove forests [49]. In this study, the combination of OBIA and RF contained two procedures: first, segmenting the NDVI-MSIC image into image objects based on an optimal image segmentation algorithm (Fig. 1c, shape, compactness, and scale were 0.17, 0.75, and 20, respectively [50]); and second, operating the RF classifier on these objects and deriving classification results of mangrove forest and others (Fig. 1d). The combination of OBIA and RF can contribute more features for classifying land covers. In addition to spectral features and indices, spatial features such as shape and texture could be used to distinguish mangrove forests and non-mangrove forests. These procedures were performed in eCognition software.

2.3. Post-processing of initial classification results

The main purpose of post-processing is to generate highly reliable classification results. First, to obtain the best interpretation, for each project task, misclassified objects were manually modified by remote sensing experts. To facilitate manual interpretation, a false color composite of MSI bands 11 (red), 8 (green), and 4 (blue) was generated [51]. As shown in Fig. 1b, in the false color composite image, mangrove forests are dark green with a smooth texture, which is significantly different from terrestrial vegetation. Then, to reduce noise, patch filtering was applied to remove small patches. Considering the patch characteristics of mangrove forests, the potential usage of the HGMF_2020 dataset, and the detectability of Sentinel-2 imagery, the threshold parameter (minimal number of pixels in a patch) was set to 6. We used 8-connectedness to identify and eliminate the isolated small patches. Thus, patches that were smaller than six 10-m resolution pixels (600 m^2) were merged with the largest patch within the 8-connected pixels.

2.4. Independent accuracy assessments

The accuracy of HGMF_2020 was validated by two independent assessment approaches, i.e., standard remote-sensing error matrix [52] and bootstrapping [53]. The bootstrapping approach is proven to be effective in validating classification datasets of coastal ecosystems. In addition to mean mapping accuracy, it provides confidence intervals (CIs) [54,55]. During the bootstrapping procedure, we took 1000 iterations to resample the samples and conducted validations. We adopted the mean of the distribution as an estimate and the 95% quantile (0.025 and 0.975 percentiles) as the corresponding CI.

In addition, our validation results indicated asymmetry between omission (1-user's accuracy) and commission (1-producer's accuracy) errors. To allow propagation of this asymmetry into our resultant areal extents, we used the 95% interval on the resampled distribution of omission and commission errors to estimate the upper and lower bounds for the areal extents of each land cover with

$$A_i 95\%\mathrm{CI}_{\mathrm{lower}} = A_i - (A_i \times \mathrm{CP}_{95}), \quad (1)$$

$$A_i 95\%\mathrm{CI}_{\mathrm{upper}} = A_i + (A \times \mathrm{OP}_{95}), \quad (2)$$

where A_i is the mapped area of the HGMF_2020 class i, and CP_{95} and OP_{95} are the 95% percentile of the commission and omission accuracies corresponding to class i, respectively.

2.5. Patch width analyses

Mangrove patches are irregular polygons, and the morphology of coastlines is uncertain; thus, directly calculating the perpendicular widths of the polygons to the coastlines is not practical. To solve this issue, we first created the largest circle inside each polygon and then selected polygons containing a circle greater than 100 or 1500 m in diameter. Thus, the selected polygons had widths exceeding 100 or 1500 m, regardless of the angles of the coastlines. Finally, we named these patches W100 and W1500, respectively.

3. Results

3.1. Accuracy of HGMF_2020

Standard error matrices and bootstrapping results are shown in Tables S1–S3 (online). The overall accuracy of HGMF_2020 was 95.2%, and the user's accuracy and producer's accuracy of mangrove forest were 91.8% and 90.3%, respectively (Table S1 online). According to the regional assessment results, the commission and omission errors of mangrove forest mapping in southeastern Asia, western Africa, and South America were higher than those in other regions (Table S2 online). The errors were mainly caused by confusing mangrove forests with lowland wetlands. In contrast, the mapping accuracies of southern Africa, southern Asia, and western Asia were much higher than those of other regions. Because the climates of these regions are relatively dry, mangrove forests are significantly different from surrounding land covers. Table S3 (online) shows 1000 iterations of bootstrapping results. The overall accuracy was 93.6% with a 95th CI of 91.4% to 95.7%, and the user's accuracy and producer's accuracy of mangrove forest are 92.0% (90.2%–93.8%, 95th CI) and 91.0% (89.6%–92.3%, 95th CI), respectively.

3.2. Area and spatial distribution of global mangrove forests in 2020

The spatial distribution and areal extent of global mangrove forests are shown in Fig. 2 and Table 1. The area of global mangrove forests was 145,068 km^2 (130,850 to 160,153 km^2, 95th CI) in 2020. Approximately 96% of mangrove forests were distributed in tropical regions (Fig. 2c). Asia had the largest amount of mangrove forests (39.2%), followed by Africa (19.3%), South America (15.4%), North America (14.3%), and Oceania (11.9%). For the United Nations (UN) statistics geographic regions [56], mangrove forests in southeastern Asia, South America, Western Africa, Central America, and Australia and New Zealand ranked the top five largest, with areal extents all exceeding 10,000 km^2 (Table 1). Fig. 2b lists the top twenty mangrove-rich countries, and these countries comprised more than 80% of the global mangrove forests. Indonesia had the largest amount of mangrove forests, followed by Brazil and Australia. Specific areas of mangrove forests in different countries are listed in Table S4 (online).

3.3. Patch size of global mangrove forests

Globally, the number of mangrove patches was 336,972 in 2020 (Fig. 3a). Asia had the largest percentage of total patch number (36.5%), followed by North America (20.8%), Oceania (18.7%), South America (12.4%), and Africa (11.6%). In total, 95% of mangrove patches were smaller than 1 km^2. For the width of global mangrove patches, 59,751 patches had a width greater than 100 m, with a sum area of 142,998 km^2, accounting for 98.5% of the global total. The number of patches with a width greater than 1500 m was 1782, with a total area of 35,831 km^2, accounting for 25% of the global total. For the United Nations (UN) statistics geographic regions, the mean patch size of Melanesia was 1.5 km^2, which was the largest, followed by Western Africa and Southern Asia, with mean patch sizes of 1.0 and 0.7 km^2, respectively. For other geographic regions, the mean patch sizes were all smaller than 0.5 km^2. Fig. 3b shows the top ten countries with the largest mean patch size. The mean patch size of mangrove forests in Bangladesh ranked the largest, followed by Congo and Cayman Is. In terms of individual patches, only 88 patches had an area larger than 100 km^2, and the largest patch was found in Everglades National Park, Florida, United States, with an area of 989 km^2 (Fig. 3c). Large patches were also found in the estuary of the Amazon River (Fig. 3d), the Sundarbans along the Bay of Bengal (Fig. 3e), and Sembilang National Park in Indonesia's South Sumatra Province (Fig. 3f).

4. Discussion

4.1. Status of global mangrove forests under conservation and threats

For years, many nongovernmental organizations, community groups, research institutions, and governmental agencies have been working globally on such efforts. For example, in 2018, the International Union for Conservation of Nature, World Wildlife Fund, Conservation International, Wetlands International, the Nature Conservancy, and many other partners formed the Global Mangrove Alliance, which aims to accelerate a coordinated and comprehensive approach for global mangrove restoration and conservation. A large number of mangrove forests are under conservation and management with intergovernmental treaties, such as the World Heritage Convention, the Convention on Biological Diversity, and the Ramsar Convention on Wetlands [15].

With efforts over the last 20 years, mangrove forests have shifted from being one of the fastest diminishing ecosystems on Earth to one of the most protected (https://www.mangrovealliance.org/mangrove-forests/). As of March 2023, 302 Ramsar sites, 23 World Heritage sites, and tens of federal or national ministry or agency reserves have been established to protect mangrove forests worldwide. As shown in Table 2 and Fig. 4a, b, mangrove forests in

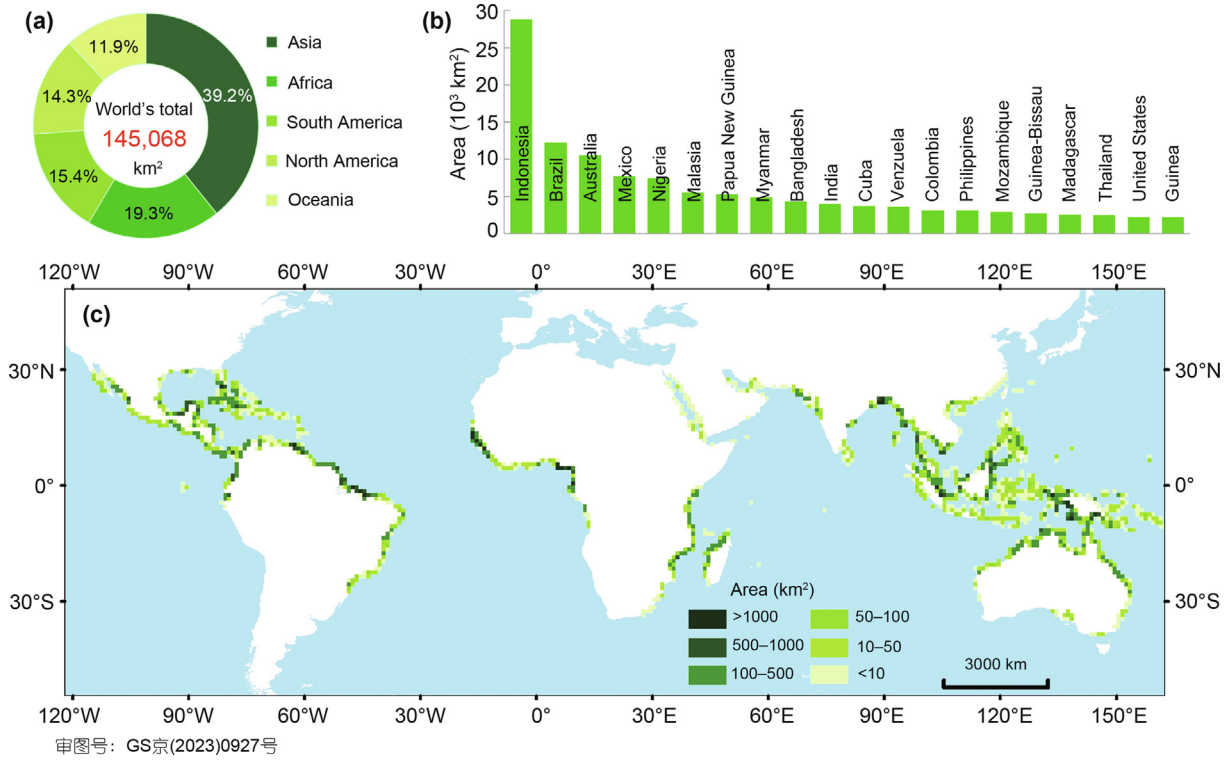

Fig. 2. Areal extent and distribution of global mangrove forests in 2020. (a) Area and proportion of mangrove forests on each continent. (b) Areal extents of mangrove forests in the top twenty mangrove-rich countries. (c) Distributions of mangrove forests summarized in each decimal degree square.

Table 1
Area of mangrove forests with 95% confidence intervals (95th CI) for each United Nations (UN) statistics geographic region.

Geographic region	Area (km^2)	95th CI (km^2)	Proportion (%)
Northern Africa	7.5	6.7–8.2	0.0
Eastern Africa	7132.2	6390.4–7831.1	4.9
Middle Africa	4137.2	3706.9–4542.7	2.9
Southern Africa	22.4	20.0–24.6	0.0
Western Africa	16,657.1	14,924.8–18,289.5	11.5
Caribbean	5518.9	4944.9–6059.7	3.8
Central America	12,715.7	11,393.3–13,961.8	8.8
Northern America	2487.8	2229.1–2731.6	1.7
South America	22,288.0	19,970.0–24,472.2	15.4
Eastern Asia	340.8	304.1–372.6	0.2
Southeastern Asia	47,008.2	42,119.3–51,615.0	32.4
Southern Asia	9333.2	8362.6–10,247.9	6.4
Western Asia	197.8	177.2–217.2	0.1
Australia and New Zealand	10,994.0	9850.7–12,071.4	7.6
Melanesia	6091.4	5457.9–6688.4	4.2
Micronesia	129.5	116.0–142.2	0.1
Polynesia	6.0	5.4–6.6	0.0

Australia were sparse, whereas natural reserves along these coasts were relatively large. In contrast, the coasts of southern and southeastern Asia had large areas of mangrove forests; however, the areal extents of mangrove forests that were protected were less.

Although more than 300 mangrove natural reserves have been established in recent decades, the conservation effectiveness of these reserves is highly variable. For positive examples, in China, mangrove forests located in the Ramsar sites and national natural reserves all recovered after the establishment of the reserves [46,57]; in Belize, due to high protection attention during 1996–2017, the annual rate of mangrove loss in the Belize Barrier Reef Reserve System (World Heritage site) was significantly lower than that outside the reserve [58]. In contrast, a series of studies indicated that there were large gaps between mangrove conservation policies and actions, and the root of mangrove degradation had been attributed to coastal economic development targets [59–62]. In Ecuador, even in protected areas, the construction of aquaculture ponds caused serious deforestation of mangrove forests [63]. In Brazil, approximately seventy percent of mangrove forests are inside protected areas; however, the strength of protection is weakened by a lack of economic interest and conservation policies [64].

Moreover, a focus only on mangrove extent could mask the degradation associated with reductions in habitat quality [15]. For example, the area of mangrove forests in the Xuan Thuy Natural Wetland, Vietnam, was relatively constant since 1989, when it was included in the List of Ramsar Wetlands of International Importance. However, in the reserve, the expansion of aquaculture

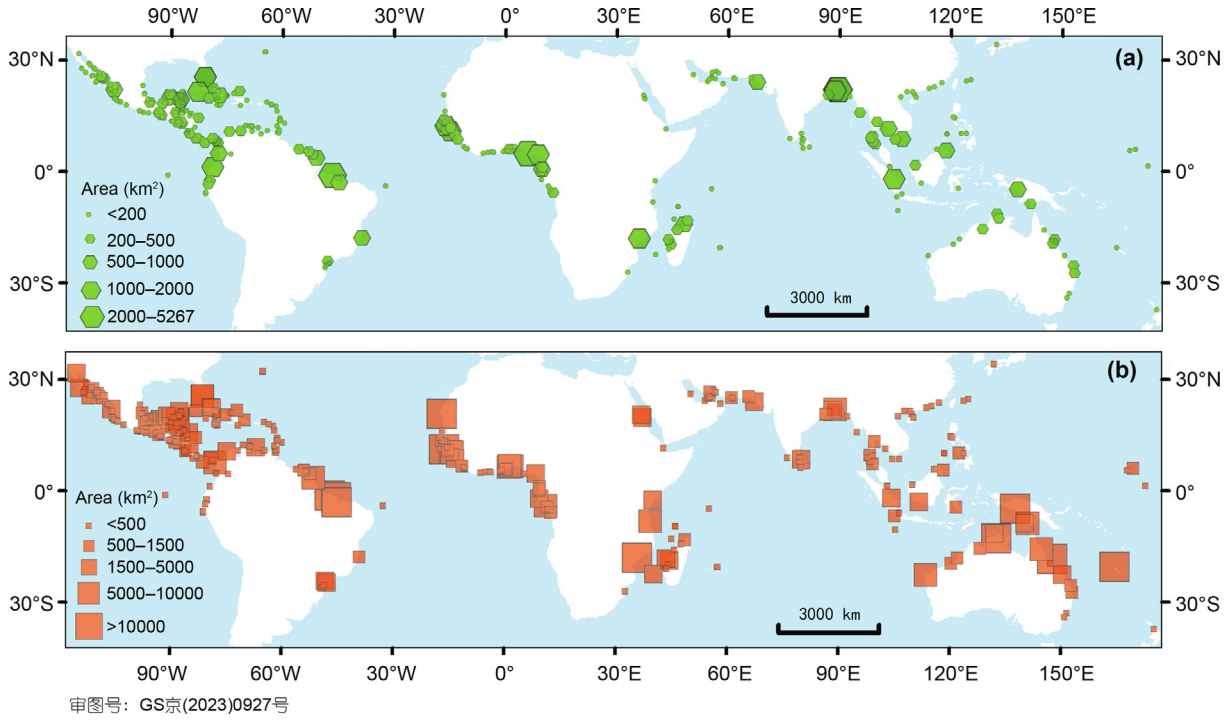

Fig. 3. Number and size of global mangrove patches and regional subsets of four large patches. (a) Number and proportion of mangrove patches on each continent. (b) Top ten countries with the largest mean mangrove patch size. Subset of the HGMF_2020 dataset overlaid on Google Earth image in Everglades National Park, Florida, the United States (c), the estuary of the Amazon River, Brazil (d), Sundarbans along the Bay of Bengal (e), and Sembilang National Park in Indonesia's South Sumatra Province (f).

Table 2
Areas and proportions of protected mangrove forests for each UN statistical geographic region.

Geographic region	Area (km^2)	Proportion (%)
Northern Africa	2.2	29.7
Eastern Africa	4028.7	56.5
Middle Africa	2554.1	61.7
Southern Africa	15.0	67.0
Western Africa	11,581.2	69.5
Caribbean	3454.4	62.6
Central America	8631.9	67.9
Northern America	1928.7	77.5
South America	13,012.8	58.4
Eastern Asia	124.1	36.5
Southeastern Asia	8958.1	19.1
Southern Asia	7150.8	76.6
Western Asia	13.7	6.9
Australia and New Zealand	2071.7	18.8
Melanesia	445.1	7.3
Micronesia	10.2	7.9
Polynesia	0.0	0.0
Global total	63,982.6	44.1

was not slowed, and the patches of mangrove forest have become fragmented [65]. Indeed, successful management, restoration, and conservation relied on the efforts of national, state, and local governments along with local communities [62]. However, due to a lack of funding and enforcement [15], local people benefited little in participating in co-management activities [66]. A previous study also indicated that financial support for mangrove protection benefits harvesters, especially by engaging local women in small business activities [66]. In addition to the World Heritage Convention, the Convention on Biological Diversity, and the Ramsar Convention on Wetlands, information provided by the HGMF_2020 dataset can be used to support a series of worldwide conservation policies, such as the UN Sustainable Development Goals (SDGs), including SDG 1 (No Poverty), SDG 2 (Zero Hunger), SDG 6 (Clean Water and Sanitation), SDG 13 (Climate Action), SDG 14 (Life under Water), and SDG 15 (Life on Land), UN Framework Convention on Climate Change, Convention on Biological Diversity, Sendai Framework on Disaster Risk Reduction, Bonn Challenge, and IUCN General Assembly and World Conservation Congress [67].

4.2. Status of mangrove forests in resisting natural disasters

Coastal zones have a large exposed population and integrated high-value assets [68]. Mangrove forests have been considered a sustainable coastal green belt to protect lives and property [42]. For example, in Kendrapada District, Orissa state, India (Fig. 5a), during the Indian super cyclone in 1999, compared to villages with narrower or no mangrove forests, villages with wider mangrove forests had significantly fewer reported deaths [69]. As we calculated from the HGMF_2020 dataset, nearly 99% of mangrove forests had a width greater than 100 m, suggesting that mangrove forests play a critical role in providing protection services globally. Fig. 5a illustrates that the W100 and W1500 mangrove patches along the coastlines of Central and South America, western Africa, and eastern and southeastern Asia protected large coastal zones. Fig. 5b shows Lagos, Nigeria, with a population over 15 million, as a typical city protected by W1500 patches. Fig. 5c shows large areas of aquaculture ponds near Hai Phong, Vietnam, which were protected by W1500 patches.

4.3. Comparisons to previous global-scale mangrove forest datasets

The HGMF_2020 is the first 10-m spatial resolution global mangrove forest dataset derived by consistent Sentinel-2 imagery and OBIA. In this section, we compared this dataset with seven remote sensing-based global-scale mangrove forest datasets (Table 3), i.e., GMFD [26], GMW v2.0, v2.5 and v3.0 [29–31], CGMFC-21 [27], LREIS_GLOBALMANGROVE, and GMF30_2000-2020. GMW v3.0 was built mainly by L-band synthetic aperture radar (SAR). The

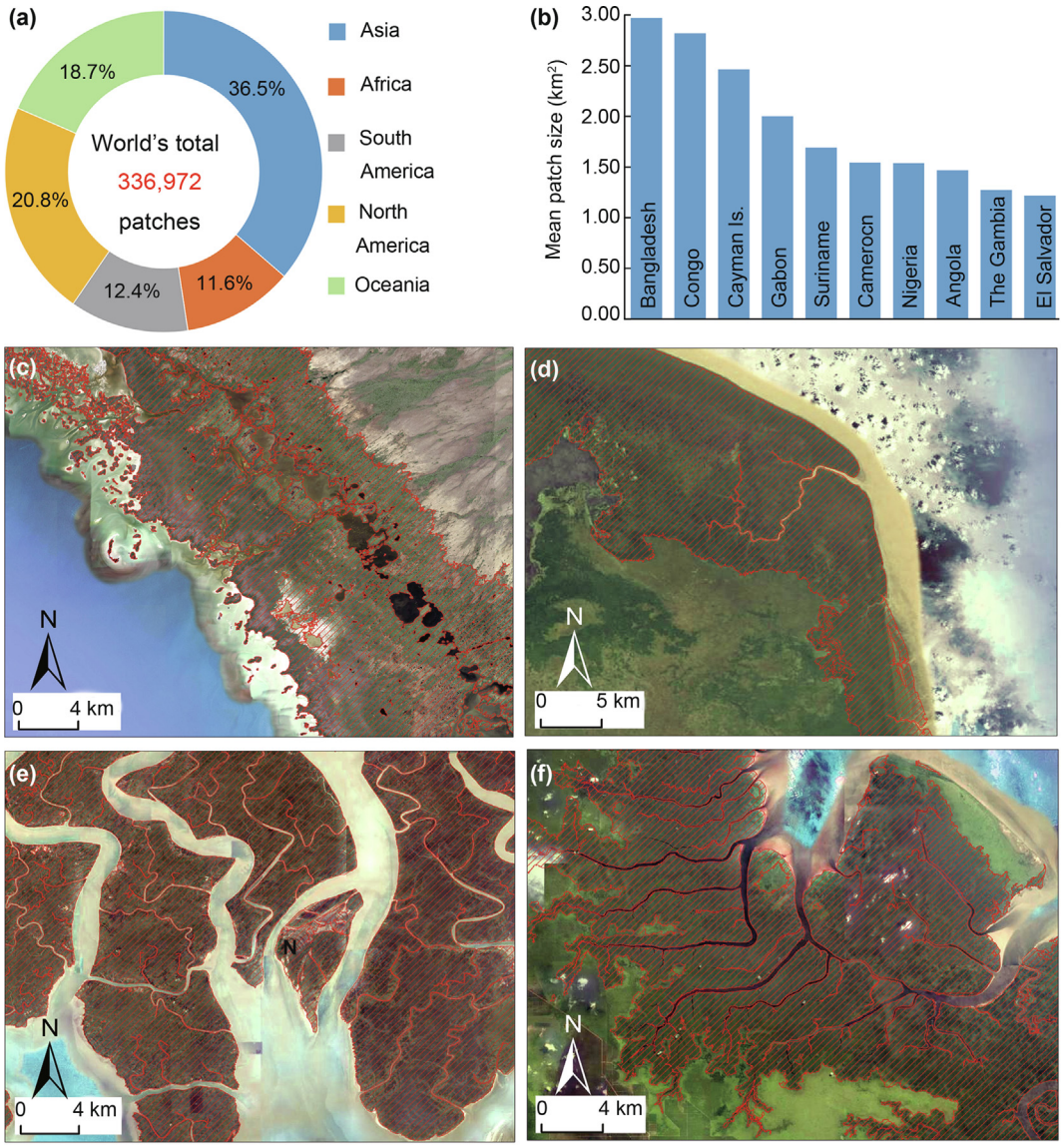

Fig. 4. Spatial information on global mangrove forest conservation. (a) Area of mangrove forests in each natural reserve. (b) Areal extent of each natural reserve, including Ramsar site, World Heritage site, and federal or national ministry or agency reserve.

other six datasets were built mainly from optical remote sensing data. For the optical-based datasets, except for CGMFC-21 and LREIS_GLOBALMANGROVE, which reported obviously larger mangrove forest extents than the others, the area of mangrove forests in HGMF_2020 was higher than the other four. The differences could be ascribed to imagery, i.e., Sentinel-2 vs. Landsat-5/7. A previous study indicated that Sentinel-2 imagery with 10-m resolution is helpful in discriminating smaller mangrove patches [30]. GMW v3.0 adopted GMW v2.5 as a baseline and detected mangrove changes using L-band SAR. However, using L-band SAR to separate mangrove forests from other woody wetlands is challenging [29–31]. Specifically, low-land wet forests adjacent to mangrove swamps could be misclassified as mangrove forests. LREIS_GLOBALMANGROVE was built by deep learning methods and Sentinel-2 between 2018 and 2020. LREIS_GLOBALMANGROVE is online shared data (https://www.scidb.cn), and as we calculated from the vector, the total area of mangrove forests was much higher than that of HGMF_2020. GMF30_2000-2020 is also an online published dataset (https://data.casearth.cn), and the total area of 2020's mangrove forests in GMF30_2000-2020 was much lower than that in HGMF_2020.

To further discuss the differences between the 10-m resolution datasets of HGMF_2020, GMW v3.0, and LREIS_GLOBALMANGROVE, three typical subsets are illustrated in Fig. 6, i.e., Bahía de Panamá, Panama (Ramsar site no. 1319, Fig. 6a–c), Apoi Creek Forests, Nigeria (Ramsar site no. 1751, Fig. 6d–f), and Lorentz National Park, Indonesia (World Heritage Site, Fig. 6g–i). As shown in Fig. 6, the superiority of the HGMF_2020 dataset can be supported based on three aspects. First, the integrity of patches in HGMF_2020 is much higher than that in the other datasets. Thus, the HGMF_2020 dataset provides geo-information that can be immediately used by scientists and managers. As shown in Fig. 6, the integrity of patches in HGMF_2020 performed better than the other two datasets. The difference can be attributed to different classification methods. GMW v3.0 was built using a pixel-based algorithm, LREIS_GLOBALMANGROVE was built based on mixed methods, and HGMF_2020 was consistently built based on OBIA. Second, HGMF_2020 delineated considerable small patches of mangrove forests, especially those along coastal edges. Therefore, HGMF_2020 can support precision management of mangrove ecosystems not only at the global scale but also at the regional and local scales. For example, HGMF_2020 contained more linear

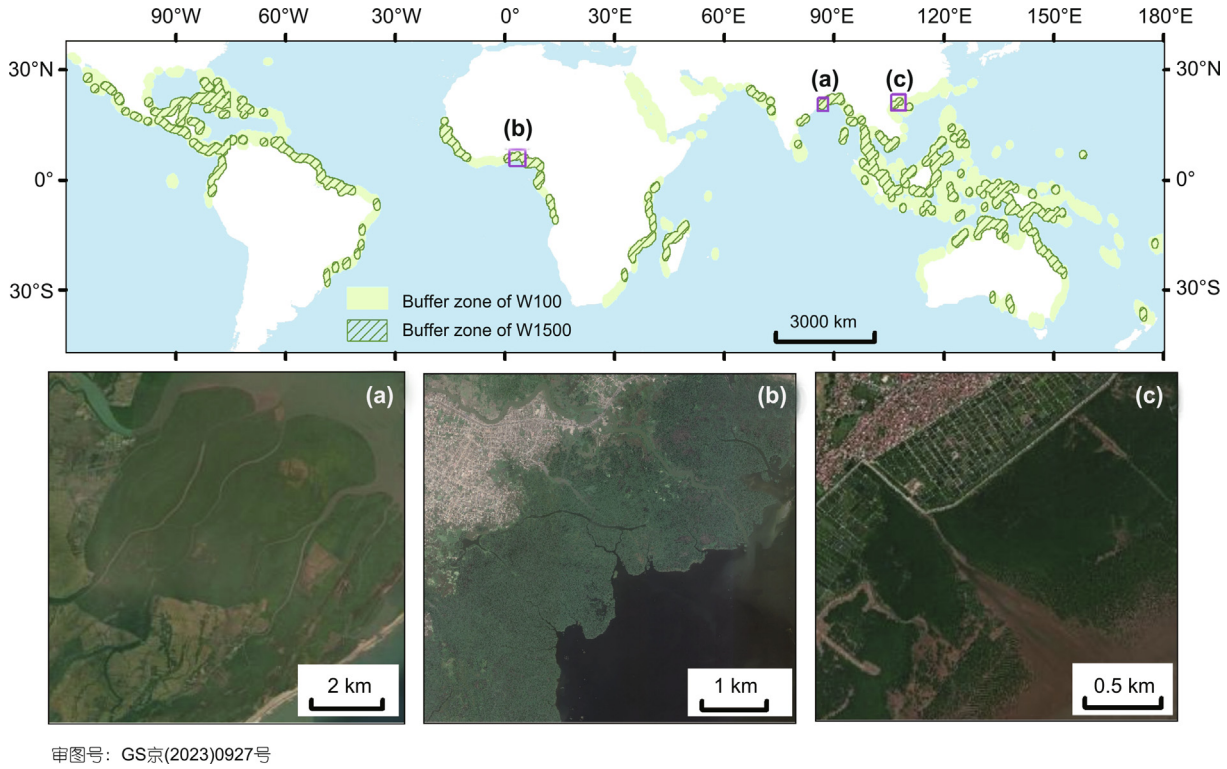

Fig. 5. 100-km buffer zone of W100 and W1500 mangrove patches. W100 and W1500 represent patches wider than 100 and 1500 m, respectively. (a) Kendrapada District, Orissa state, India. (b) Lagos, Nigeria, protected by W1500 patches. (c) Aquaculture ponds protected by W1500 patches in Hai Phong, Vietnam.

Table 3
Areas of mangrove forests in HGMF_2020 and other remote sensing-based global-scale datasets.

Dataset	Reference year	Data source	Resolution (m)	Areas (km^2)
HGMF_2020	2020	Sentinel-2 MSI	10	145,068
GMFD	2000	Landsat-TM/ETM+	30	137,760
GMW v2.0	2010	ALOS PALSAR	30	137,600
GMF30_2000-2020	2020	Landsat-TM/ETM+ Landsat-TM/OLI	30	113,779
GMW v2.5	2010	Landsat TM/ETM+ ALOS PALSAR Sentinel-2 MSI	10–30	140,260
GMW v3.0	2020	ERS-1 SAR ALOS PALSAR ALOS-2 PALSAR-2	25	147,359
CGMFC-21	2012	Landsat-TM/ETM+	30	167,387
LREIS_GLOBALMANGROVE	2020	Sentinel-2 MSI	10	168,659

patches outside aquaculture ponds. Third, HGMF_2020 contained reasonable geographical spatial details. As shown in the subset of Lorentz National Park (Fig. 6g–i), mangrove patches in HGMF_2020 were split only by tidal creeks (Fig. 6g), whereas unreasonable noise widely existed in the patches of the other two.

4.4. Reliability, updateability and uncertainties of the HGMF_2020 dataset

The reliability of the HGMF_2020 database could be attributed to three factors, i.e., the higher spatial resolution of Sentinel-2 imagery, the robust images obtained by MSIC, and the better performance of OBIA. First, compared to Landsat imagery, the finer spatial resolution of Sentinel-2 imagery offers great opportunities to obtain mangrove patches with more spatial details. Second, the MSIC overcomes the uncertainties derived from tidal variations within a scene. Third, the OBIA has advantages over pixel-based classification because it uses spectral, textural, and neighborhood information during classification and generally produces higher accuracy [70,71] and reduces salt-and-pepper effects [72]. Therefore, the classification result can be directly used for further analysis.

Compared to previous global mangrove forest databases, the advantages of the HGMF_2020 database not only lie in the higher spatial resolution but also the addition of information on patch patterns. Owing to this advantage, the HGMF_2020 database has more potential to support a range of policy mechanisms, such as informing global policy frameworks about trends in mangrove health and distribution, identifying drivers of loss and recovery, mapping mangrove values, and setting and monitoring targets for conservation and rehabilitation.

In addition, HGMF_2020 is an updatable dataset. The current availability of advanced satellite imagery allows for the acquisition of rapid and robust updatable products, especially Sentinel-2 imagery, which has a short revisit cycle of 2–5 days. The GEE platform enabled swift processes of a large number of satellite images across

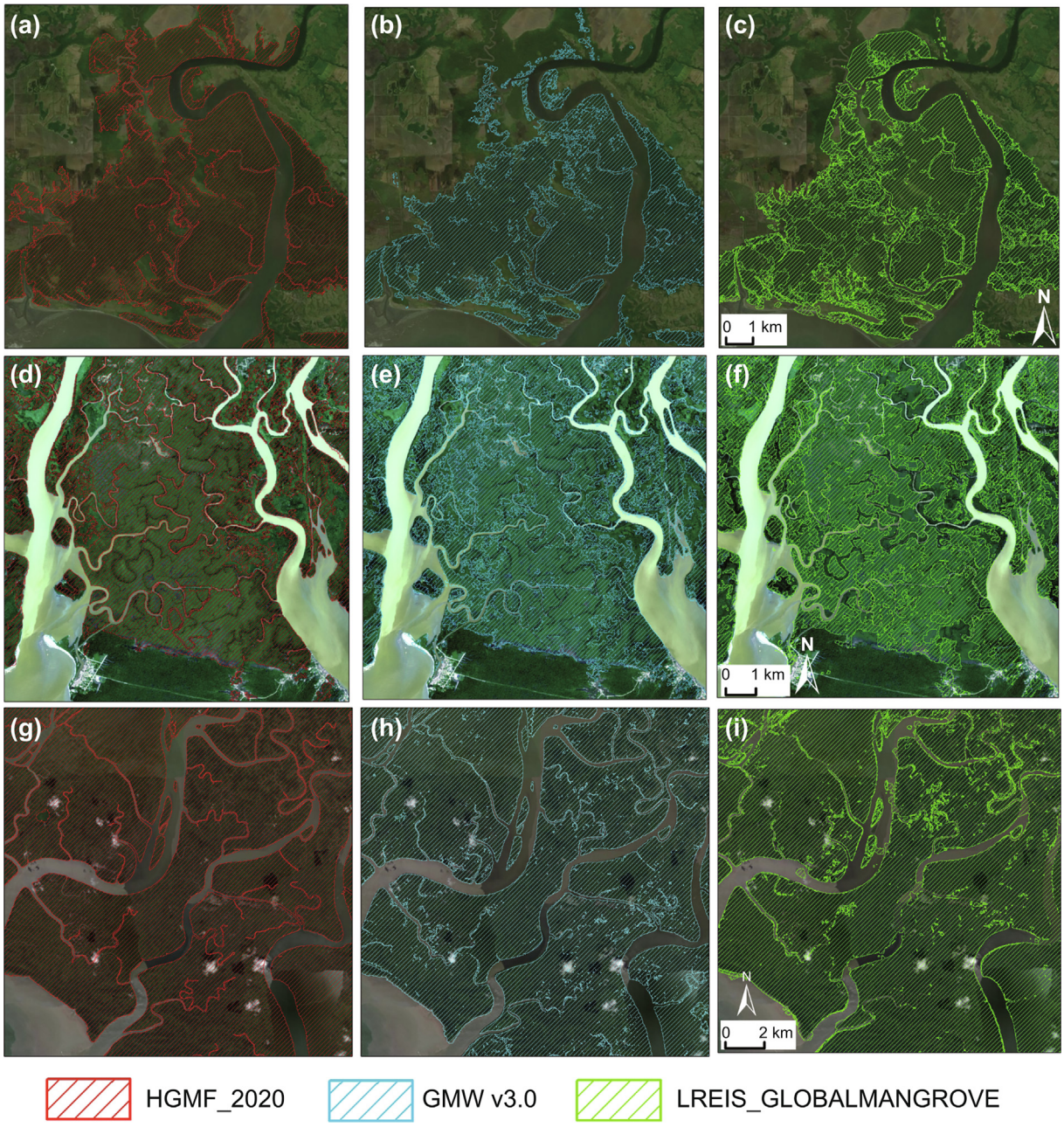

Fig. 6. Typical subsets of HGMF_2020, GMW v3.0, and LREIS_GLOBALMANGROVE in Bahía de Panamá, Panama (Ramsar site no. 1319. (a) HGMF_2020; (b) GMW v3.0; (c) LREIS_GLOBALMANGROVE), Apoi Creek Forests, Nigeria (Ramsar site no. 1751. (d) HGMF_2020; (e) GMW v3.0; (f) LREIS_GLOBALMANGROVE), and Lorentz National Park, Indonesia (World Heritage site. (g) HGMF_2020; (h) GMW v3.0; (i) LREIS_GLOBALMANGROVE).

large scales [73]. The HGMF_2020 dataset can be updated annually by applying image classifications only to locations with changes.

Uncertainties in HGMF_2020 were mainly caused by three factors. First, commission errors were caused by misclassification with lowland wet forests. For example, in Lorentz National Park, lowland wet forests with spectral and texture features similar to those of mangrove forests are directly connected to mangrove forests, and thus, they are difficult to differentiate from mangrove forests. Second, data gaps emerged from cloud coverage. Although NDVI-MSIC has great potential to remove cloud pixels, clouds may still exist in small regions. Third, due to the spatial resolution of Sentinel-2 imagery and the capacity of the OBIA, the minimum mapping unit of HGMF_2020 was set to 600 m^2 (six 10-m resolution pixels); thus, smaller patches could not be identified or mapped.

5. Conclusion

Up-to-date information and assessment of mangrove forests distributions and patch structures are essential in supporting the implementation of relevant sustainable management. This study produced the first 10-m resolution dataset of global mangrove forests, i.e., HGMF_2020, which contains the abovementioned information. Based on the HGMF_2020 dataset, we conducted further analysis of the status of global mangrove forests from different perspectives. From the perspective of ecosystem conservation and threats, mangrove forests located on the coasts of western Africa had a better status due to the higher proportion of conservation and larger area of natural reserves; in contrast, mangrove forests in eastern and southeastern Asia were in a disadvantageous situation due to the lower proportion of conservation and

vast extent of anthropogenic land cover. From the perspective of resisting natural disasters, mangrove forests in southern, eastern and southeastern Asia, Northern America, and western Africa greatly contributed to protecting properties due to the larger patch size. This study presents a quantitative analysis of global mangrove forests status in association with conservation, threats, and coastal protection. HGMF_2020, with consistent spatial and temporal fine resolution, offers the critical baseline for evaluating the role of mangrove forests toward sustainability and the assessment of SDGs.

Conflict of interest

The authors declare that they have no conflict of interest.

Acknowledgments

This work was jointly supported by the Open Research Program of the International Research Center of Big Data for Sustainable Development Goals (CBAS2022ORP06), the Strategic Priority Research Program of Chinese Academy of Sciences (XDA19040500), the National Natural Science Foundation of China (42171372 and 42171379), the Youth Innovation Promotion Association of Chinese Academy of Sciences (2021227), the Open Fund of State Laboratory of Information Engineering in Surveying, Mapping and Remote Sensing, Wuhan University (19I02), and the National Earth System Science Data Center (www.geodata.cn). Xiangming Xiao was supported by the U.S. National Science Foundation (1911955).

Author contributions

Mingming Jia and Zongming Wang designed the research, processed the data, and wrote the draft. Yeqiao Wang contributed to designing the research and reviewing the manuscript. Dehua Mao, Chunying Ren, and Kaishan Song contributed to image analysis and reviewing the manuscript. Chao Wang and Chuanpeng Zhao contributed to image analysis, fieldwork, and reviewing the manuscript. Xiangming Xiao contributed to reviewing the manuscript.

Appendix A. Supplementary materials

Supplementary materials to this article can be found online at https://doi.org/10.1016/j.scib.2023.05.004.

Data availability

The authors declare that the main data supporting the findings of this work are available within the article and its Supplementary materials. The code of creating and downloading Sentinel-2 composite images is also available at Google Earth Engine (GEE) platform via: https://code.earthengine.google.com/856b74cbdcfaea690bcf5f72648b48c2. Spatial distributions of global mangrove forests in HGMF_2020 are visible at GEE platform via: https://jiam m6128.users.earthengine.app/view/hgmf2020. The dataset of HGMF_2020 can be downloaded freely through Harvard Dataverse: https://doi.org/10.7910/DVN/PKAN93.

References

[1] Field C, Osborn J, Hoffman L, et al. Mangrove biodiversity and ecosystem function. Glob Ecol Biogeogr Lett 1998;7:3–14.
[2] Alongi DM. Carbon cycling and storage in mangrove forests. Annu Rev Mar Sci 2014;6:195–219.
[3] Wang Y, Bonynge G, Nugranad J, et al. Remote sensing of mangrove change along the Tanzania coast. Mar Geod 2003;26:35–48.
[4] Menéndez P, Losada IJ, Beck MW, et al. Valuing the protection services of mangroves at national scale: the Philippines. Ecosyst Serv 2018;34:24–36.
[5] Menéndez P, Losada IJ, Torres-Ortega S, et al. The global flood protection benefits of mangroves. Sci Rep 2020;10:4404.
[6] Marois DE, Mitsch WJ. Coastal protection from tsunamis and cyclones provided by mangrove wetlands—a review. Int J Biodivers Sci Ecosyst Serv Manage 2015;11:71–83.
[7] Alongi DM. Carbon sequestration in mangrove forests. Carbon Manage 2012;3:313–22.
[8] Lee SY, Primavera JH, Dahdouh-Guebas F, et al. Ecological role and services of tropical mangrove ecosystems: a reassessment. Glob Ecol Biogeogr 2014;23:726–43.
[9] Zhang C, Shi T, Liu J, et al. Eco-engineering approaches for ocean negative carbon emission. Sci Bull 2022;67:2564–73.
[10] Duke N, Nagelkerken I, Agardy T, et al. The importance of mangroves to people: a call to action. Cambridge: United Nations Environment Programme World Conservation Monitoring Centre (UNEP-WCMC); 2014.
[11] Friess DA, Yando ES, Alemu JB, et al. Ecosystem services and disservices of mangrove forests and salt marshes. Oceanogr Mar Biol 2020;58:107–42.
[12] Mukherjee N, Sutherland WJ, Dicks L, et al. Ecosystem service valuations of mangrove ecosystems to inform decision making and future valuation exercises. PLoS One 2014;9:e107706.
[13] Fakhruddin B, Mahalingam R, Padmanaban R. Sustainable development goals for reducing the impact of sea level rise on mangrove forests. Indian J Geo-Mar Sci 2018;47:1947–58.
[14] Food and Agriculture Organization of the United Nations. The world's mangroves 1980–2005. FAO Forestry Paper 2007;153. 77.
[15] Friess DA, Rogers K, Lovelock CE, et al. The state of the world's mangrove forests: past, present, and future. Annu Rev Env Resour 2019;44:89–115.
[16] Wang L, Jia M, Yin D, et al. A review of remote sensing for mangrove forests: 1956–2018. Remote Sens Environ 2019;231:111223.
[17] Wilkie ML, Fortuna S. Status and trends in mangrove area extent worldwide. Forest Resources Assessment Programme Working Paper (FAO), 2003.
[18] Saenger P, Hegerl E, Davie JD. Global status of mangrove ecosystems. International Union for Conservation of Nature and Natural Resources; 1983.
[19] Lanly J, Clement J. Tropical forest resources assessment project (in the framework of the global environment monitoring system—GEMS). Forest resources of tropical Africa. Pt. I: regional synthesis. Technical Report, 1981.
[20] Fisher P, Spalding M. Protected areas with mangrove habitat. Cambridge: World Conservation Centre; 1993.
[21] Food and Agriculture Organization of the United Nations. Global forest resources assessment 2020: main report. 2020.
[22] Lu Y, Wang L. How to automate timely large-scale mangrove mapping with remote sensing. Remote Sens Environ 2021;264:112584.
[23] Lu Y, Wang L. The current status, potential and challenges of remote sensing for large-scale mangrove studies. Int J Remote Sens 2022;43:6824–55.
[24] Spalding M. World atlas of mangroves. London and Washington DC: Earthscan; 2010.
[25] Spalding M, Blasco F, Field C. World mangrove atlas. Okinawa: The International Society for Mangrove Ecosystems; 1997.
[26] Giri C, Ochieng E, Tieszen LL, et al. Status and distribution of mangrove forests of the world using Earth observation satellite data: status and distributions of global mangroves. Glob Ecol Biogeogr 2011;20:154–9.
[27] Hamilton SE, Casey D. Creation of a high spatio-temporal resolution global database of continuous mangrove forest cover for the 21st century (CGMFC-21). Glob Ecol Biogeogr 2016;25:729–38.
[28] Thomas N, Lucas R, Bunting P, et al. Distribution and drivers of global mangrove forest change, 1996–2010. PLoS One 2017;12:e0179302.
[29] Bunting P, Rosenqvist A, Lucas R, et al. The global mangrove watch—a new 2010 global baseline of mangrove extent. Remote Sens 2018;10:1669.
[30] Bunting P, Rosenqvist A, Hilarides L, et al. Global mangrove watch: updated 2010 mangrove forest extent (v2.5). Remote Sens 2022;14:1034.
[31] Bunting P, Rosenqvist A, Hilarides L, et al. Global mangrove extent change 1996-2020: Global Mangrove Watch Version 3.0. Remote Sens 2022;14:3657.
[32] Li M, Chen B, Webster C, et al. The land-sea interface mapping: China's coastal land covers at 10 m for 2020. Sci Bull 2022;67:1750–4.
[33] Goldberg L, Lagomasino D, Thomas N, et al. Global declines in human-driven mangrove loss. Glob Chang Biol 2020;26:5844–55.
[34] Hutchison J, Manica A, Swetnam R, et al. Predicting global patterns in mangrove forest biomass. Conserv Lett 2013;7:233–40.
[35] Tang W, Zheng M, Zhao X, et al. Big geospatial data analytics for global mangrove biomass and carbon estimation. Sustainability 2018;10:472.
[36] Bryan-Brown DN, Connolly RM, Richards DR, et al. Global trends in mangrove forest fragmentation. Sci Rep 2020;10:7117.
[37] Alongi DM. The impact of climate change on mangrove forests. Curr Clim Chang Rep 2015;1:30–9.
[38] Feller IC, Friess DA, Krauss KW, et al. The state of the world's mangroves in the 21st century under climate change. Hydrobiologia 2017;803:1–12.
[39] Richards DR, Friess DA. Rates and drivers of mangrove deforestation in Southeast Asia, 2000–2012. Proc Natl Acad Sci USA 2016;113:344–9.
[40] Ward RD, Friess DA, Day RH, et al. Impacts of climate change on mangrove ecosystems: a region by region overview. Ecosyst Health Sust 2016;2:e01211.

[41] Alongi DM. Mangrove forests: resilience, protection from tsunamis, and responses to global climate change. Estuar Coast Shelf Sci 2008;76:1–13.
[42] Mazda Y, Magi M, Ikeda Y, et al. Wave reduction in a mangrove forest dominated by *Sonneratia* sp. Wetl Ecol Manage 2006;14:365.
[43] Hashim AM, Catherine SMP. Effectiveness of mangrove forests in surface wave attenuation: a review. Res J Appl Sci Eng Technol 2013;5:4483–5448.
[44] Mazda Y, Magi M, Kogo M, et al. Mangroves as a coastal protection from waves in the Tong King delta. Viet Mangroves Salt Marshes 1997;1:127–35.
[45] Jia M, Wang Z, Zhang Y, et al. Monitoring loss and recovery of mangrove forests during 42 years: the achievements of mangrove conservation in China. Int J Appl Earth Obs Geoinf 2018;73:535–45.
[46] Jia M, Wang Z, Mao D, et al. Spatial-temporal changes of China's mangrove forests over the past 50 years: an analysis towards the Sustainable Development Goals (SDGs). Chin Sci Bull 2021;66:3886–901 (in Chinese).
[47] Tucker CJ. Red and photographic infrared linear combinations for monitoring vegetation. Remote Sens Environ 1979;8:127–50.
[48] Jia M, Mao D, Wang Z, et al. Tracking long-term floodplain wetland changes: a case study in the China side of the Amur River Basin. Int J Appl Earth Obs Geoinf 2020;92:102185.
[49] Li H, Jia M, Zhang R, et al. Incorporating the plant phenological trajectory into mangrove species mapping with dense time series Sentinel-2 imagery and the Google Earth Engine platform. Remote Sens 2019;11:2479.
[50] Zhang R, Jia M, Wang Z, et al. A comparison of Gaofen-2 and Sentinel-2 imagery for mapping mangrove forests using object-oriented analysis and random forest. IEEE J Sel Top Appl Earth Observ Remote Sens 2021;14:4185–93.
[51] Jia M, Wang Z, Li L, et al. Mapping China's mangroves based on an object-oriented classification of Landsat imagery. Wetlands 2014;34:277–83.
[52] Champagne C, McNairn H, Daneshfar B, et al. A bootstrap method for assessing classification accuracy and confidence for agricultural land use mapping in Canada. Int J Appl Earth Obs Geoinf 2014;29:44–52.
[53] Efron B, Tibshirani R. Improvements on cross-validation: the 632+ bootstrap method. J Am Stat Assoc 1997;92:548–60.
[54] Murray NJ, Phinn SR, DeWitt M, et al. The global distribution and trajectory of tidal flats. Nature 2019;565:222–5.
[55] Murray NJ, Worthington TA, Bunting P, et al. High-resolution mapping of losses and gains of Earth's tidal wetlands. Science 2022;376:744–9.
[56] United Nations. Standard country or area codes for statistical use. 1999.
[57] Mao D, Wang Z, Wang Y, et al. Remote observations in China's Ramsar Sites: wetland dynamics, anthropogenic threats, and implications for sustainable development goals. J Remote Sens 2021;2021:1–13.
[58] Cherrington EA, Griffin RE, Anderson ER, et al. Use of public Earth observation data for tracking progress in sustainable management of coastal forest ecosystems in Belize. Cent Am Remote Sens Environ 2020;245:111798.
[59] Friess DA, Thompson BS, Brown B, et al. Policy challenges and approaches for the conservation of mangrove forests in Southeast Asia. Conserv Biol 2016;30:933–49.
[60] Nguyen HH, Nguyen CT, Dai VN. Spatial-temporal dynamics of mangrove extent in Quang Ninh Province over 33 years (1987–2020): implications toward mangrove management in Vietnam. Reg Stud Mar Sci 2022;52:102212.
[61] Chaudhuri P, Ghosh S, Bakshi M, et al. A review of threats and vulnerabilities to mangrove habitats: with special emphasis on east coast of India. J Earth Sci Clim Chang 2015;6:1000270.
[62] Romañach SS, DeAngelis DL, Koh HL, et al. Conservation and restoration of mangroves: global status, perspectives, and prognosis. Ocean Coast Manage 2018;154:72–82.
[63] López-Rodríguez F. Mangrove in Ecuador: conservation and management strategies, coastal environments. London: IntechOpen; 2021.
[64] Ferreira AC, Lacerda LD. Degradation and conservation of Brazilian mangroves, status and perspectives. Ocean Coast Manage 2016;125:38–46.
[65] Seto KC, Fragkias M. Mangrove conversion and aquaculture development in Vietnam: a remote sensing-based approach for evaluating the Ramsar Convention on Wetlands. Glob Environ Change 2007;17:486–500.
[66] Begum F, Bruyn LL, Kristiansen P, et al. Institutionalising co-management activities for conservation of forest resources: evidence from the Sundarban mangrove forest management of Bangladesh. J Environ Manage 2021;298:113504.
[67] Worthington TA, Andradi-Brown DA, Bhargava R, et al. Harnessing big data to support the conservation and rehabilitation of mangrove forests globally. One Earth 2020;2:429–43.
[68] Li G, Li X, Yao T, et al. Heterogeneous sea-level rises along coastal zones and small islands. Sci Bull 2019;64:748–55.
[69] Das S, Vincent JR. Mangroves protected villages and reduced death toll during Indian super cyclone. Proc Natl Acad Sci USA 2009;106:7357–60.
[70] Aguilar MA, Nemmaoui A, Novelli A, et al. Object-based greenhouse mapping using very high resolution satellite data and Landsat 8 time series. Remote Sens 2016;8:513.
[71] Gilbertson JK, Kemp J, Van NA. Effect of pan-sharpening multi-temporal Landsat 8 imagery for crop type differentiation using different classification techniques. Comput Electron Agric 2017;134:151–9.
[72] Jia M, Liu M, Wang Z, et al. Evaluating the effectiveness of conservation on mangroves: a remote sensing-based comparison for two adjacent protected areas in Shenzhen and Hong Kong. China Remote Sens 2016;8:627.
[73] Wang L, Diao C, Xian G, et al. A summary of the special issue on remote sensing of land change science with Google Earth Engine. Remote Sens Environ 2020;248:112002.

Mingming Jia is an associate professor at Northeast Institute of Geography and Agroecology, Chinese Academy of Sciences. Her research interest focuses on remote sensing of mangrove wetlands and delivering the science necessary to inform local-to-global scale environment management and conservation. She has several ongoing research projects about quantifying changes of mangrove wetlands and its impacts on global biodiversity conservation, carbon sequestration, and UN's Sustainable Development Goals implementation.

Zongming Wang is a professor of Northeast Institute of Geography and Agroecology, Chinese Academy of Sciences. He works at the interface of remote sensing, geospatial science and ecology. His research interest focuses on remote sensing of wetlands, remote sensing of ecosystem services, and conservation and restoration of wetland ecosystems. He is the chair of Remote Sensing Society of Jilin Province, and a founding chair of the Conference on Remote Sensing of Wetlands.

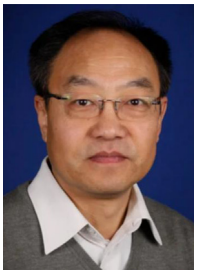

Yeqiao Wang is a professor of terrestrial remote sensing at the Department of Natural Resources Science, University of Rhode Island, USA. He is particularly interested in remote sensing of dynamics of landscape and land change science. His research projects include mapping and monitoring changes of ecological conditions in different spatial and temporal scales of coastal environments, wetlands, mountainous regions, protected areas, and urban landscapes, in order to improve understanding of intertwined human and natural systems, and the sustainability, vulnerability, resilience of land and water resources.